

- variability of the deeper components of the slope water. Although variability of the deep components of this system is expected on NAO time scales (3, 5), there is no clear mechanism linking the NAO and the surface slope water current.
3. R. R. Dickson *et al.*, *Prog. Oceanogr.* **38**, 241 (1996).
  4. J. W. Hurrell, *Science* **269**, 676 (1995).
  5. S. Bacon, *Nature* **394**, 871 (1999).
  6. K. Skene, thesis, Dalhousie University (1998).
  7. D. J. W. Piper and K. Skene, *Paleoceanography* **13**, 205 (1998).
  8. Samples were extruded from the core tubes, sliced into 1-cm layers, and bagged. Subsamples were taken for micropaleontological study of the fraction >150  $\mu\text{m}$  and for percent carbonate analysis with an automated gasometric technique. Sediment color was measured with a Coloron spectrophotometer and is presented using the "Lab" system [*CIE Colorimetry* **15.2** (1986)].
  9. L. D. Keigwin, *Science* **274**, 1504 (1996).
  10. As discussed in (17) and elsewhere [D. O. Suman and M. P. Bacon, *Deep-Sea Res.* **36**, 869 (1989)], Holocene carbonate cycles on the Bermuda Rise are driven mostly by pulses in the flux of terrigenous silts and clays.
  11. The red clay-rich sediments that compose this facies are thought to derive from subglacial turbidite flow out of the Gulf of St. Lawrence [D. A. V. Stow, *Am. Assoc. Petrol. Geol.* **65**, 375 (1981)]. On the Scotian Margin, about half the glacial maximum to modern sedimentary section is this red sediment (22), and its thickness is even greater on the fan (7).
  12. Accelerator mass spectrometer (AMS)  $^{14}\text{C}$  measurements (Table 1) were made at the National Ocean Sciences AMS facility at Woods Hole on mixed planktonic foraminifera. Ages were converted to calendar years, according to Stuiver and Reimer [M. Stuiver and P. J. Reimer, *Radiocarbon* **35**, 215 (1993)], with a reservoir correction of 440 years. Age models were based on a linear fit of the ages to depth. For MC-25 the data are nearly linear, whereas for MC-13 there are age reversals of up to a few hundred years (Table 1). For this core, the age model is assumed to be linear from the origin to the deepest dated sample. Any other reasonable age model for MC-13 and MC-25 would still correctly identify the LIA near the core top, but ages of events deeper than about 10 cm in these cores are probably not known to better than  $\pm 200$  years.
  13. The relationship between percent *N. pachyderma* data from North Atlantic core tops and SST was presented by Kohfeld *et al.* (15). They showed that *N. pachyderma* blooms in the summer at high latitudes, whereas the only time series data on *N. pachyderma* growth in subpolar locations showed that the bloom occurs in the spring [L. R. Sautter and R. C. Thunell, *J. Foram. Res.* **19**, 253 (1989)].
  14. W. L. Balsam and F. W. McCoy Jr., *Paleoceanography* **2**, 531 (1987).
  15. K. Kohfeld *et al.*, *ibid.* **11**, 679 (1996).
  16. Although we do not have chronologies for these cores, the maximum percent *N. pachyderma* is found at the 3-cm level in each: 56% at MC-19 and 41% at MC-21.
  17. L. D. Keigwin and G. A. Jones, *Deep-Sea Res.* **36**, 845 (1989); L. D. Keigwin and G. A. Jones, *J. Geophys. Res.* **99**, 12,397 (1994).
  18. G. Bond *et al.*, *Science* **278**, 1257 (1997).
  19. G. G. Bianchi and I. N. McCave, *Nature* **397**, 515 (1999).
  20. E. P. Laine and C. D. Hollister, *Mar. Geol.* **39**, 277 (1981).
  21. C. Appenzeller *et al.*, *Science* **282**, 446 (1998).
  22. L. D. Keigwin and G. A. Jones, *Paleoceanography* **10**, 973 (1995).
  23. R. S. Pickart and W. M. Smethie Jr., *Deep-Sea Res.* **45**, 1053 (1998).
  24. *Oceanus* cruise 326 and this research were funded by the National Science Foundation. We thank L. A. Conroy, K. Elder, C. E. Franks, J. Kelleher, E. Roosen, D. Torres, and the staff of the National Ocean Sciences AMS Facility for their assistance; R. Schmitt, I. N. McCave, and D. Oppo for reading the manuscript; and N. Driscoll, J. Grotzinger, and M. McCartney for helpful discussions.

29 June 1999; accepted 25 August 1999

## Multiple Ink Nanolithography: Toward a Multiple-Pen Nano-Plotter

Seunghun Hong, Jin Zhu, Chad A. Mirkin\*

The formation of intricate nanostructures will require the ability to maintain surface registry during several patterning steps. A scanning probe method, dip-pen nanolithography (DPN), can be used to pattern monolayers of different organic molecules down to a 5-nanometer separation. An "overwriting" capability of DPN allows one nanostructure to be generated and the areas surrounding that nanostructure to be filled in with a second type of "ink."

Recently, there has been an intense effort to develop micro- and nanolithographic methods analogous to macroscopic writing and printing tools (1-4). These methods are allowing researchers to address important issues in biology (5) and molecule-based electronics (6-9). Microcontact printing (2-4) and even micropen writing (1) have been successful in terms of preparing molecule-based structures on the  $\sim 100$ -nm to centimeter length scale. We recently showed that dip-pen nanolithography (DPN) allows one to prepare custom, "single-ink" structures with dimensions on the sub-100 nm length scale (10). A significant issue in efforts to prepare nanolithographic printing tools pertains to registry—that is, how to use multiple inks within the context of one set of nanostruc-

tures spaced nanometers apart. At present, stamping procedures do not have the resolution capabilities of scanning probe lithographic methods or electron-beam (e-beam) methods, and with respect to multiple inks, they pose significant alignment problems (4). Moreover, traditional high-resolution techniques (11-24), such as electron and ion beam lithography and many scanning probe methods, rely on resist layers and the backfilling of etched areas with component molecules. These indirect patterning approaches can compromise the chemical purity of the structures generated and pose limitations on the types of materials and number of different materials that can be patterned. Indeed, adsorbate-adsorbate exchange can be problematic because a monolayer resist, which has surface binding functionality identical to that in the ink, is typically used in these methods (18).

We report the generation of multicomponent nanostructures by DPN (10) and show that chemically pristine patterns of multiple different materials can be generated with near-perfect alignment and 5-nm spatial separation.

Additionally, we report an overwriting capability of DPN that allows one to generate a nanostructure and then fill in areas surrounding that nanostructure with a second type of ink. These demonstrations are analogous to the transition from (single ink) conventional printing to "four-color" printing, and should open many opportunities for those interested in studying molecule-based electronics, catalysis, and molecular diagnostics. Indeed, the spatial resolution of this multiple ink technique is similar to the length scale of conventional large organic molecules and many biomolecules (nucleic acids and proteins).

DPN relies on a water meniscus, which in air naturally forms between the tip and sample, as the ink transport medium, and therefore, one can use relative humidity as one method of control over ink transport rate, feature size, and linewidth (10, 25, 26). Before our invention of DPN, others attempted to develop scanning probe methods for depositing organic materials on solid substrates (27). They demonstrated deposition of micrometer-scale features composed of physisorbed multilayers of 1-octadecanethiol (ODT) on mica but concluded that under the conditions used ODT could not be transported to Au and, apparently, did not recognize the importance of humidity and the meniscus in the transport process. All DPN experiments were carried out with a ThermoMicroscopes CP AFM and conventional cantilevers (ThermoMicroscopes sharpened Microlever A, force constant = 0.05 N/m). To minimize piezo tube drift problems, we used a 100- $\mu\text{m}$  scanner with closed loop scan control for all of the experiments. The ink in a DPN experiment can be loaded by using a solution method, which was described previously (10), or by using a vapor deposition

Department of Chemistry and NU Center for Nanofabrication and Molecular Self-Assembly, Northwestern University, 2145 Sheridan Road, Evanston, IL 60208, USA.

\*To whom correspondence should be addressed. E-mail: camirkin@chem.nwu.edu

## REPORTS

method for liquids and low-melting point solids. The latter involves suspending the silicon nitride cantilever in a 100-ml reaction vessel 1 cm above the ink of interest. The system is closed, heated at 60°C for 20 min, and then allowed to cool to room temperature before use. Scanning electron microscopy analyses of tips before and after ink coating by solution or vapor deposition methods show that the inks uniformly coat the tips. The uniform coatings on these tips allow one to deposit adsorbate in a controlled manner as well as to obtain high-quality images. For example, 70-nm letters with 15-nm linewidths can be drawn on Au(111) by moving the tip along the substrate (2 nm/s speed, contact force  $\sim 0.1$  nN, relative humidity  $\sim 23\%$ ) (Fig. 1). Imaging is done by increasing the scan size and imaging both patterned and unpatterned areas with the modified tip (contact force  $\sim 0.1$  nN, scan speed = 5 Hz, relative humidity  $\sim 23\%$ ). Direct deposition of self-assembled monolayers (SAMs) on this scale has not been demonstrated by any other technique, and in view of the radius of curvature ( $\sim 10$  nm) for Microlever A, this scale likely represents the linewidth resolution limit for DPN with this type of tip. However, it should be noted that an increase in DPN resolution may be possible by using sharper tips (such as nanotubes) (28–30).

The ability of DPN to form and image nanostructures offers the prospect of generating nanostructures made of different soft materials with high registry. The basic idea for generating multiple patterns in registry by DPN is related to analogous strategies for generating multicomponent structures by e-beam lithography that rely on alignment marks. However, DPN has two distinct advantages: (i) It does not make use of resists, and (ii) it uses the scanning probe for generating and locating alignment marks. The latter is important because it is less destructive than e-beam methodology for finding alignment marks (that is, it is compatible with soft materials), and it is an inherently higher resolution imaging technique than the optical or

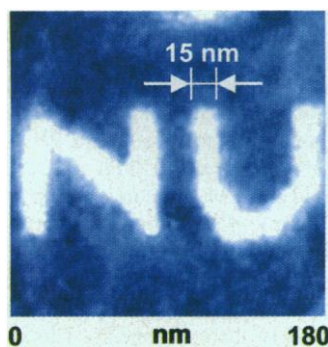


**Fig. 1.** Nanoscale molecular letters written on an Au(111) surface with MHA molecules by DPN.

e-beam methods.

We demonstrated the registration capabilities of DPN by generating a pattern of 15-nm-diameter, SAM dots of 16-mercaptohexadecanoic acid (MHA) on one of the atomically flat terraces of an Au(111) substrate (Fig. 2A). Each dot was formed by holding an MHA-coated tip in contact (contact force  $\sim 0.1$  nN, relative humidity  $\sim 23\%$ ) with the Au(111) surface for 10 s. By increasing the scan size, the patterned dots are then imaged with the same tip by lateral force microscopy (LFM); because the SAM and bare Au have very different wetting properties, LFM provides excellent contrast (31). Based on the position of the first pattern, the coordinates of additional patterns can be determined (Fig. 2B) for the precise placement of a second pattern of MHA dots. The uniformity and 5-nm spatial separation of the dots is apparent (Fig. 2A). The elapsed time between generating the data in Fig. 2, A and C, was 10 min, demonstrating near perfect nanostructure alignment with a thermal drift of less than 1 nm/min under ambient conditions.

The method that we have developed for

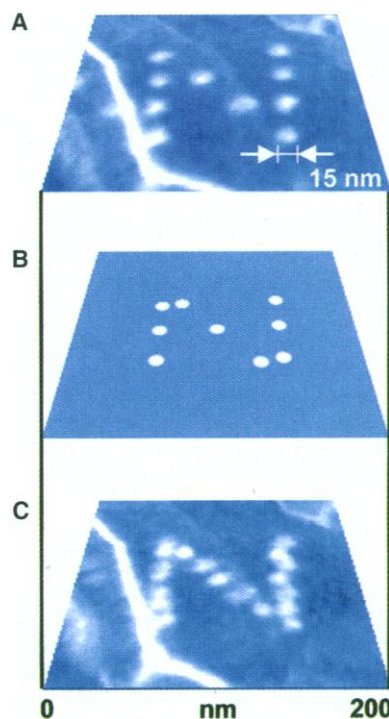


**Fig. 2.** Schematic diagram with LFM images of nanoscale molecular dots showing the essential requirements for patterning and aligning multiple nanostructures by DPN. (A) A pattern of 15-nm-diameter MHA dots on Au(111) imaged by LFM with an MHA-coated tip. (B) Anticipated placement of the second set of MHA dots as determined by calculated coordinates based on the positions of the first set of dots. (C) Image after a second pattern of MHA nanodots has been placed within the first set of MHA dots. The white jagged line is an Au(111) grain boundary.

generating pristine multiple ink nanostructures in registry with one another required an additional modification of the experiment described above and in Fig. 2. Because the MHA SAM dot patterns were imaged with an ink-coated tip, it is likely that a small amount of undetectable ink is deposited in the unpatterned area while imaging. Such deposition could significantly affect some applications of patterned materials prepared by DPN, especially those dealing with electronic measurements on molecule-based structures. To overcome this problem, we make use of micrometer-scale alignment marks drawn with an MHA-coated tip (cross-hairs in Fig. 3A, contact force  $\sim 0.1$  nN, scan speed = 4 Hz, relative humidity  $\sim 30\%$ ) to precisely place nanostructures on the Au substrate without cross-ink contamination. In a typical experiment, we draw an initial pattern of 50-nm parallel lines (contact force  $\sim 0.1$  nN, scan speed = 4 Hz) composed of MHA and separated by 190 nm (Fig. 3A). This pattern is 2  $\mu\text{m}$  away from the exterior alignment marks. An image of these lines is not taken with the MHA-coated tip to avoid contamination of the patterned area. The tip is then replaced with an ODT-coated tip. This tip is used to locate the alignment marks (not the first set of lines), and then precalculated coordinates

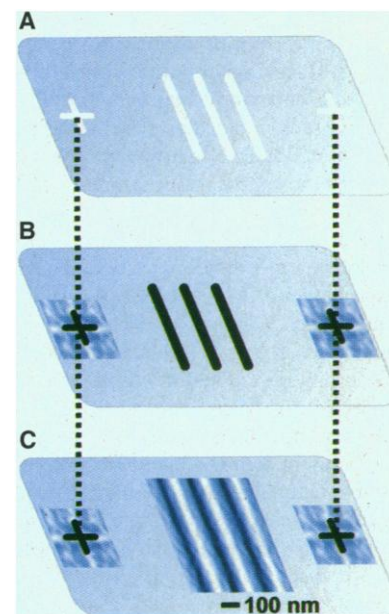


**Fig. 3.** Diagram depicting the method for generating aligned soft nanostructures. (A) The first pattern is generated with MHA (denoted by white lines), along with microscopic alignment marks (cross-hairs), by DPN. The actual lines are not imaged to preserve the pristine nature of the nanostructure. (B) The second set of parallel lines is generated with ODT molecules, on the basis of coordinates calculated from the positions of the alignment marks in (A). (C) LFM image of the interdigitated 50-nm-wide lines separated by 70 nm.

based on the position of the alignment marks (Fig. 3B) are used to pattern the substrate with a second set of 50-nm parallel ODT SAM lines (contact force  $\sim 0.1$  nN, scan speed = 4 Hz) (Fig. 3C). These lines are placed in interdigitated manner and with near perfect registry with respect to the first set of MHA SAM lines (Fig. 3C).

An additional capability of DPN, which we refer to as "overwriting," involves generating one soft structure out of one type of ink and then filling in with a second type of ink by raster scanning across the original nanostructure. Because water is the transport medium in the DPN experiment and the water solubilities of the inks used in these experiments are very low, there is no detectable exchange between the molecules used to generate the nanostructure and the ones used to overwrite on the exposed gold (Fig. 4). We used a MHA-coated tip to generate three geometric structures, a triangle (80-nm linewidth, 30-s writing time per side), square (60-nm linewidth, 20-s writing time per side), and pentagon (30-nm linewidth, 8-s writing time per side) (contact force  $\sim 0.1$  nN, scan speed = 4 Hz, relative humidity  $\sim 35\%$ ). The tip was then changed, and a  $3 \mu\text{m}$  by  $3 \mu\text{m}$  area that comprised the original nanostructures was overwritten with an ODT-coated tip by raster scanning four times across the substrate (contact force  $\sim 0.1$  nN, scan speed = 4 Hz). Increasing the scan size to  $4.3 \mu\text{m}$  by  $4.3 \mu\text{m}$  and imaging the patterned areas with an uncoated tip (contact force  $\sim 0.1$  nN, scan speed = 5 Hz, relative humidity  $\sim 35\%$ ) shows the MHA-patterned areas (white, high friction), the ODT-overwritten areas (dark blue, low friction), and the surrounding unmodified Au (light blue, medium friction).

The multiple ink capabilities of DPN will offer opportunities to begin studying the interactions between highly sophisticated, multicomponent nanostructures and molecules in solution or the gas phase on a scale that was previously unattainable. Moreover, they will empower those in the field of molecule-based electronics to generate and evaluate custom-

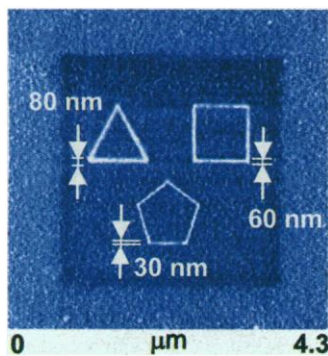


**Fig. 4.** SAMs in the shapes of polygons drawn by DPN with MHA on an amorphous Au surface. An ODT SAM has been overwritten around the polygons.

ized multicomponent soft nanostructures that are interfaced with macroscopically addressable circuitry.

#### References and Notes

1. A. Kumar, H. A. Biebuyck, N. L. Abbott, G. M. Whitesides, *J. Am. Chem. Soc.* **114**, 9188 (1992).
2. D. W. Wang, S. G. Thomas, K. L. Wang, Y. Xia, G. M. Whitesides, *Appl. Phys. Lett.* **70**, 1593 (1997).
3. R. J. Jackman, J. L. Wilbur, G. M. Whitesides, *Science* **269**, 664 (1995).
4. Y. Xia, J. A. Rogers, K. E. Paul, G. M. Whitesides, *Chem. Rev.* **99**, 1823 (1999).
5. C. S. Chen, M. Mrksich, S. Huang, G. M. Whitesides, D. E. Ingber, *Biotechnol. Prog.* **14**, 356 (1998).
6. M. A. Reed, C. Zhou, C. J. Muller, T. P. Burgin, J. M. Tour, *Science* **278**, 252 (1997).
7. R. P. Andres *et al.*, *ibid.* **272**, 1323 (1996).
8. D. L. Feldheim and C. D. Keating, *Chem. Soc. Rev.* **27**, 1 (1998).
9. L. A. Bumm *et al.*, *Science* **271**, 1705 (1996).
10. R. D. Piner, J. Zhu, F. Xu, S. Hong, C. A. Mirkin, *ibid.* **283**, 661 (1999).
11. J. K. Schoer and R. M. Crooks, *Langmuir* **13**, 2323 (1997).
12. C. S. Whelan, M. J. Lercel, H. G. Graighead, K. Seshadri, D. L. Allara, *Appl. Phys. Lett.* **69**, 4245 (1996).
13. R. Younk *et al.*, *ibid.* **71**, 1261 (1997).
14. L. A. Bottomley, *Anal. Chem.* **70**, 425R (1998).
15. R. M. Nyffenegger and R. M. Penner, *Chem. Rev.* **97**, 1195 (1997).
16. K. K. Berggren *et al.*, *Science* **269**, 1255 (1995).
17. J. A. M. Sondaghuethorst, H. R. J. van Helleputte, L. G. J. Fokink, *Appl. Phys. Lett.* **64**, 285 (1994).
18. S. Xu and G. Y. Liu, *Langmuir* **13**, 127 (1997).
19. F. K. Perkins *et al.*, *Appl. Phys. Lett.* **68**, 550 (1996).
20. D. W. Carr *et al.*, *J. Vac. Sci. Technol. A* **15**, 1446 (1997).
21. H. Sugimura and N. Nakagiri, *ibid.* **14**, 1223 (1996).
22. T. Komeda, K. Namba, Y. Nishioka, *ibid.* **16**, 1680 (1998).
23. H. U. Muller, C. David, B. Volkel, M. Grunze, *J. Vac. Sci. Technol. B* **13**, 2846 (1995).
24. Y. Kim and C. M. Lieber, *Science* **257**, 375 (1992).
25. R. D. Piner and C. A. Mirkin, *Langmuir* **13**, 6864 (1997).
26. Supplementary material is available at [www.sciencemag.org/feature/data/1044170.shl](http://www.sciencemag.org/feature/data/1044170.shl).
27. M. Jaschke and H. J. Butt, *Langmuir* **11**, 1061 (1995).
28. S. S. Wong, J. D. Harper, P. T. Lansbury Jr., C. M. Lieber, *J. Am. Chem. Soc.* **120**, 603 (1998).
29. H. J. Dai, J. H. Hafner, A. G. Rinzler, D. T. Colbert, R. E. Smalley, *Nature* **384**, 147 (1996).
30. J. C. Rosa, *Appl. Phys. Lett.* **73**, 2684 (1998).
31. J. L. Wilbur, H. A. Biebuyck, J. C. MacDonald, G. M. Whitesides, *Langmuir* **11**, 825 (1995).
32. This work was supported by the Air Force Office of Scientific Research and National Science Foundation-funded NU Materials Research Center. A. Taton, G. Mitchell, R. P. Van Duynne, and G. Whitesides are acknowledged for helpful discussions.

3 August 1999; accepted 9 September 1999

## $\beta$ -Defensins: Linking Innate and Adaptive Immunity Through Dendritic and T Cell CCR6

D. Yang,<sup>1</sup> O. Chertov,<sup>2</sup> S. N. Bykovskaia,<sup>3</sup> Q. Chen,<sup>1</sup> M. J. Buffo,<sup>3</sup> J. Shogan,<sup>3</sup> M. Anderson,<sup>4</sup> J. M. Schröder,<sup>5</sup> J. M. Wang,<sup>1</sup> O. M. Z. Howard,<sup>2</sup> J. J. Oppenheim<sup>1\*</sup>

Defensins contribute to host defense by disrupting the cytoplasmic membrane of microorganisms. This report shows that human  $\beta$ -defensins are also chemotactic for immature dendritic cells and memory T cells. Human  $\beta$ -defensin was selectively chemotactic for cells stably transfected to express human CCR6, a chemokine receptor preferentially expressed by immature dendritic cells and memory T cells. The  $\beta$ -defensin-induced chemotaxis was sensitive to pertussis toxin and inhibited by antibodies to CCR6. The binding of iodinated LARC, the chemokine ligand for CCR6, to CCR6-transfected cells was competitively displaced by  $\beta$ -defensin. Thus,  $\beta$ -defensins may promote adaptive immune responses by recruiting dendritic and T cells to the site of microbial invasion through interaction with CCR6.

Defensins, a family of small (3.5 to 4.5 kD) cationic antimicrobial peptides with three to four intramolecular cysteine disulfide bonds,

are found in mammals, insects, and plants (1–4). On the basis of the position and bonding of six conserved cysteine residues, defensins in vertebrates are divided into two categories, designated as  $\alpha$ - and  $\beta$ -defensins (1, 2). Unlike  $\alpha$ -defensins that are produced by neutrophils and intestinal Paneth cells,  $\beta$ -defensins are primarily expressed by epithelial cells of the skin, kidneys, and tracheobronchial lining of nearly all vertebrates, where they can be released upon microbial invasion or up-regulated by stimulation with lipopolysaccharide and tumor necrosis factor- $\alpha$  (TNF- $\alpha$ ) (2, 5, 6). Two types of human  $\beta$ -defensins (HBDs),  $\beta$ -defensins 1 and 2

<sup>1</sup>Laboratory of Molecular Immunoregulation, Division of Basic Sciences, <sup>2</sup>Intramural Research Support Program, SAIC Frederick, National Cancer Institute–Frederick Cancer Research and Development Center, Frederick, MD 21702–1201, USA. <sup>3</sup>Allegheny University of Health Sciences, Pittsburgh, PA 15212, USA. <sup>4</sup>Magainin Research Institute, 5110 Campus Drive, Plymouth Meeting, PA 19642, USA. <sup>5</sup>Department of Dermatology, Christian Albrechts University of Kiel, Schittenhelmstrasse 7, D-24105 Kiel, Germany.

\*To whom correspondence should be addressed. E-mail: [oppenhei@mail.ncifcrf.gov](mailto:oppenhei@mail.ncifcrf.gov)

## LINKED CITATIONS

- Page 1 of 2 -



You have printed the following article:

### **Multiple Ink Nanolithography: Toward a Multiple-Pen Nano-Plotter**

Seunghun Hong; Jin Zhu; Chad A. Mirkin

*Science*, New Series, Vol. 286, No. 5439. (Oct. 15, 1999), pp. 523-525.

Stable URL:

<http://links.jstor.org/sici?sici=0036-8075%2819991015%293%3A286%3A5439%3C523%3AMINTAM%3E2.0.CO%3B2-3>

---

This article references the following linked citations:

## References and Notes

### <sup>3</sup> **Fabrication of Submicrometer Features on Curved Substrates by Microcontact Printing**

Rebecca J. Jackman; James L. Wilbur; George M. Whitesides

*Science*, New Series, Vol. 269, No. 5224. (Aug. 4, 1995), pp. 664-666.

Stable URL:

<http://links.jstor.org/sici?sici=0036-8075%2819950804%293%3A269%3A5224%3C664%3AFOSFOC%3E2.0.CO%3B2-R>

### <sup>6</sup> **Conductance of a Molecular Junction**

M. A. Reed; C. Zhou; C. J. Muller; T. P. Burgin; J. M. Tour

*Science*, New Series, Vol. 278, No. 5336. (Oct. 10, 1997), pp. 252-254.

Stable URL:

<http://links.jstor.org/sici?sici=0036-8075%2819971010%293%3A278%3A5336%3C252%3ACOAMJ%3E2.0.CO%3B2-B>

### <sup>9</sup> **Are Single Molecular Wires Conducting?**

L. A. Bumm; J. J. Arnold; M. T. Cygan; T. D. Dunbar; T. P. Burgin; L. Jones II; D. L. Allara; J. M. Tour; P. S. Weiss

*Science*, New Series, Vol. 271, No. 5256. (Mar. 22, 1996), pp. 1705-1707.

Stable URL:

<http://links.jstor.org/sici?sici=0036-8075%2819960322%293%3A271%3A5256%3C1705%3AASMWC%3E2.0.CO%3B2-Z>

### <sup>16</sup> **Microlithography by Using Neutral Metastable Atoms and Self-Assembled Monolayers**

Karl K. Berggren; Andreas Bard; James L. Wilbur; John D. Gillaspay; Andreas G. Helg; Jabez J. McClelland; Steven L. Rolston; William D. Phillips; Mara Prentiss; George M. Whitesides

*Science*, New Series, Vol. 269, No. 5228. (Sep. 1, 1995), pp. 1255-1257.

Stable URL:

<http://links.jstor.org/sici?sici=0036-8075%2819950901%293%3A269%3A5228%3C1255%3AMBUNMA%3E2.0.CO%3B2-3>

**NOTE:** The reference numbering from the original has been maintained in this citation list.

## LINKED CITATIONS

- Page 2 of 2 -



<sup>24</sup> **Machining Oxide Thin Films with an Atomic Force Microscope: Pattern and Object Formation on the Nanometer Scale**

Yun Kim; Charles M. Lieber

*Science*, New Series, Vol. 257, No. 5068. (Jul. 17, 1992), pp. 375-377.

Stable URL:

<http://links.jstor.org/sici?sici=0036-8075%2819920717%293%3A257%3A5068%3C375%3AMOTFWA%3E2.0.CO%3B2-B>